

# A Finite Element Model to Investigate the Impact of Torch Angle on an Autogenous TIG Welding Process

Richard Turner

PRISM<sup>2</sup> Research Group, School of Metallurgy & Materials, University of Birmingham, Birmingham, UK

Email: r.p.turner@bham.ac.uk

**How to cite this paper:** Turner, R. (2017) A Finite Element Model to Investigate the Impact of Torch Angle on an Autogenous TIG Welding Process. *World Journal of Engineering and Technology*, 5, 743-753. <https://doi.org/10.4236/wjet.2017.54062>

**Received:** October 25, 2017

**Accepted:** November 25, 2017

**Published:** November 28, 2017

Copyright © 2017 by author and Scientific Research Publishing Inc. This work is licensed under the Creative Commons Attribution International License (CC BY 4.0).

<http://creativecommons.org/licenses/by/4.0/>



Open Access

## Abstract

A numerical modelling activity was completed to explore the impact that the angle  $\theta$  created by the torch from the vertical had upon the thermal and mechanical predictions for a T-joint autogenous TIG welded component. A parametric system of 9 models was set-up to simulate the effects of varying the angle  $\theta$  by a small, potentially unnoticeable amount to a manual operator. The variations ranged from  $-8^\circ$  to  $+8^\circ$  away from a nominal default position of torch. The numerical models were created and computed using specialist welding simulation software Sysweld, and pre/post-processing software Visual Environment (both owned by ESI Group). The resulting weakly-coupled thermal and mechanical analyses illustrated a small deflection of angle that the weld bead was penetrating in to the T-joint, consistent with the variation in torch angle, and a negligible variation in peak temperature of 1.8%. The mechanical results however demonstrated a more significant output, namely that the distortion observed upon the vertical plate within the T-joint was predicted to increase by over 50% as result of this small shift in the welding torch angle. However, other mechanical predictions for plastic strain, Von Mises residual stress and distortion on the horizontal plate, were all suggesting only very minor sensitivity (typically less than 5%) to the torch angle variation. However, the predictions for vertical plate distortions demonstrate how difficult a manual TIG operation can be to perform with sufficient process control and repeatability, due to the significant impact that human operator-induced variation has upon some of the mechanical outputs.

## Keywords

Arc Welding, Distortion, Von Mises Residual Stress, Plastic Strain

## 1. Introduction

A substantial number of industrially used Tungsten-inert Gas (TIG) welding cells remain manual-operated—meaning that a trained TIG welder will manually hold the torch and move it along its prescribed weld path. Whereas, newer TIG welding cells are fully automated and use a robot arm to position and move the torch relative to the weld path during the welding operation, thus improving the process repeatability [1]. The manual cells do therefore add extra uncertainty surrounding human operator repeatability. The angle of the torch during an autogenous TIG welding operation is defined as  $\theta$  in the below figure. This angle that the torch is positioned at is an input parameter that is easily varied in an experimental set-up, but also one for which small variations may be totally unconsidered by an operator. TIG welding does remain one of the most common forms of forming a welding for thin sectioned joints across a number of industries, due to its low cost and its wide applicability [2] [3].

Computational weld mechanics has been widely studied across the literature, notably amongst the academic community [4] [5] [6], which allows for detailed parametric investigations of the various input parameters used within a process, to allow for greater understanding to be gained surrounding these parameter effects and sensitivities, process optimization and component assessment without the need to carry out potentially expensive, time-consuming experimental trials to gain the same information. By setting up of a relatively simple computational weld model, the effects of a single parameter can easily be explored. Parametric-designed computational weld models, identical in every input except for the parameter of interest, can then be created and computed reasonably quickly, to allow for an assessment of the influence of this individual parameter upon the predicted outcomes from the welding model. Similar numerical and computational finite element modelling of other fusion welding operations (e.g.: Electron Beam [7], laser [8], MIG welding [9], hybrid welding methods [10]) have been researched within academia and industry for a considerable number of years, and as such defined three-dimensional functions have been developed to describe the distribution of the heat in to a section of material, to represent the interaction between heat source and weldment. These include the Gaussian function [11], double ellipsoid (Goldak) function [12] and conical function. For typical older arc-welding methods, the double ellipsoid function is often used.

In this paper, a sensitivity study matrix was set up to investigate the impact upon thermal loading and mechanical distortion caused by small variations in the torch angle, at  $2^\circ$  increments, up to  $\pm 8^\circ$  from a default position, upon a titanium alloy T-joint weld (**Figure 1**). Thus in this paper,  $\theta = 0^\circ$  describes a pre-defined torch angle to consider as a baseline. Whilst a large-scale change of angle would predictably have a significant impact upon both the thermal and mechanical results, focusing upon a much narrower range of torch angle variation will allow the modeller to identify the predicted sensitivity in results which may be achieved by unintentional and simple process/operator variance.

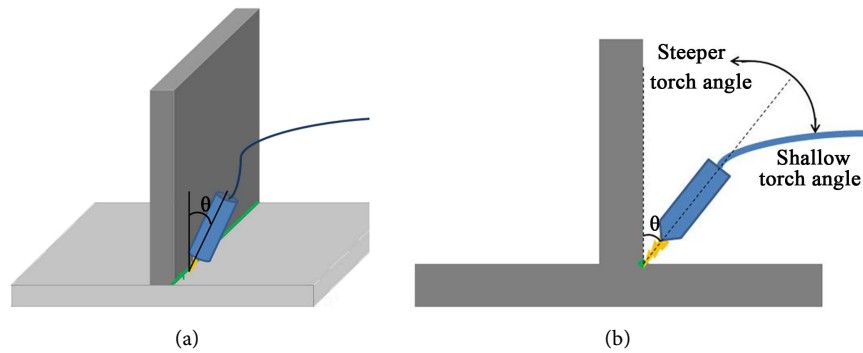


**Figure 1.** A schematic showing the parameter “torch angle” for (a) an isometric 3D view and (b) a 2D cross-section representation of a T-joint.

## 2. Modelling Methodology

The specialist welding Finite element simulation code Sysweld (v2014) from software developers ESI Group [13], has been used to perform the numerical calculations. The model itself was built within the ESI pre-processor units, Visual Weld and Visual Mesh, both part of the Visual Environment suite of Finite Element tools. A 2D mesh containing elements at the interface region measuring 0.25 mm in length, and coarsening away from the interface to elements of 2.7 mm in length, was prepared. This mesh was then swept in the 3rd dimension, along which the weld path would be placed, using a constant element edge length of 2 mm (see Figure 2). This reflects the need within FE weld simulation for the finer element sizes to be located close to the weld, and finest in the directions perpendicular to the travel direction.

A material model is applied to the elements to represent a titanium alloy of interest. A weld line is created at the 90° interface between the horizontal and vertical plates. Relevant rigid body clamps are applied, to represent the physical constraints of the welding set-up. Finally, a row of elements at the interface between the 2 plates is converted to a subtly different material model from the rest of the titanium material, one with a very low stiffness to allow for the flexibility of motion between the plates [6] [14]. Time-stepping of the model is set such that each time-step allows the TIG heat source to progress 1 element length (2 mm) in the welding direction. Once the models have computed, they can be interrogated within another of the Visual Environment 9.5 FE tools, called Visual Viewer. The nine models created are then given process parameters as described in Table 1.

## 3. Finite Element Predictions & Discussion

The nine simulated TIG welding passes were then studied for the trends they displayed to highlight the impact of changing the angle with which the TIG torch is held by the operator by a small, unnoticeable amount by the operator. These results are now considered in three distinct sections, a) Thermal predictions, b) distortion predictions and c) Residual stress predictions. A summary of all the modelling predictions are presented in Table 2.

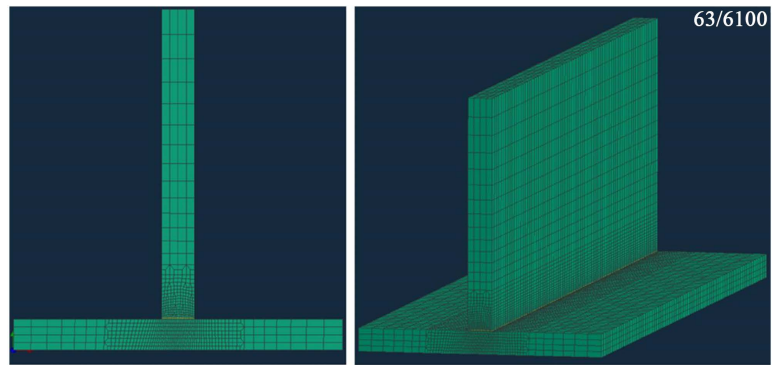


**Figure 2.** The 2D mesh created describing the cross-section of the T-joint to be modelled, and the resulting 3D mesh when swept through in to the welding direction. Image taken using ESI Visual Environment pre-processing software.

**Table 1.** Matrix of parameters used in the sensitivity study. Note only the torch angle varies.

Torch Angle (°)	Welding Parameters Used		
	Weld Speed (mm/s)	Energy per Unit length (J/mm)	Efficiency
-8	20	700	0.7
-6	20	700	0.7
-4	20	700	0.7
-2	20	700	0.7
Default	20	700	0.7
2	20	700	0.7
4	20	700	0.7
6	20	700	0.7
8	20	700	0.7

**Table 2.** Predicted results from the 9 models considering welding torch angle sensitivity study.

Torch Angle (°)	FE modelling predictions (Peak values)				
	Peak Temperature (°C)	distortion on horizontal plate (mm)	distortion on vertical plate (mm)	Von Mises residual stress (MPa)	Plastic strain (-)
-8	2141	0.456	0.245	943	0.455
-6	2152	0.450	0.266	943	0.460
-4	2160	0.446	0.289	943	0.475
-2	2165	0.442	0.311	941	0.471
Default	2171	0.439	0.331	938	0.484
2	2177	0.437	0.351	936	0.480
4	2181	0.435	0.373	936	0.506
6	2182	0.434	0.395	933	0.505
8	2181	0.432	0.417	930	0.506

### 3.1. Thermal

The Sysweld outputted predictions are split in to the thermo-metallurgical predictions, which consider the thermal loading upon the component, and the weakly-coupled mechanical results, which use the thermal calculations to predict the mechanical response in terms of deformation, residual stress and plastic strain. Analysing the thermal results, unsurprisingly there is only a small variation in the angle which the molten pool penetrates the weld section. However, as the angle varies, so does the depth to which the molten pool penetrates.

Due to the similarity of thermal results (see **Figure 3**), not all nine of the modelled thermal results are shown, only those for the minimum torch angle ( $-8^\circ$ ), the default torch angle (Default) and maximum torch angle ( $+8^\circ$ ). However, the peak recorded temperature inside the weld pool is shown for all models in **Figure 4**.

It can be seen in **Figure 4** that only a very minor sensitivity in peak temperature is observed, with the maximum temperature sensitivity recorded at 1.8%, thus giving no concern that a small perturbation in the torch angle significantly changes thermal results—as would be expected. The small variations are likely caused by numerical issues concerning the position of element integration points within the heat source.

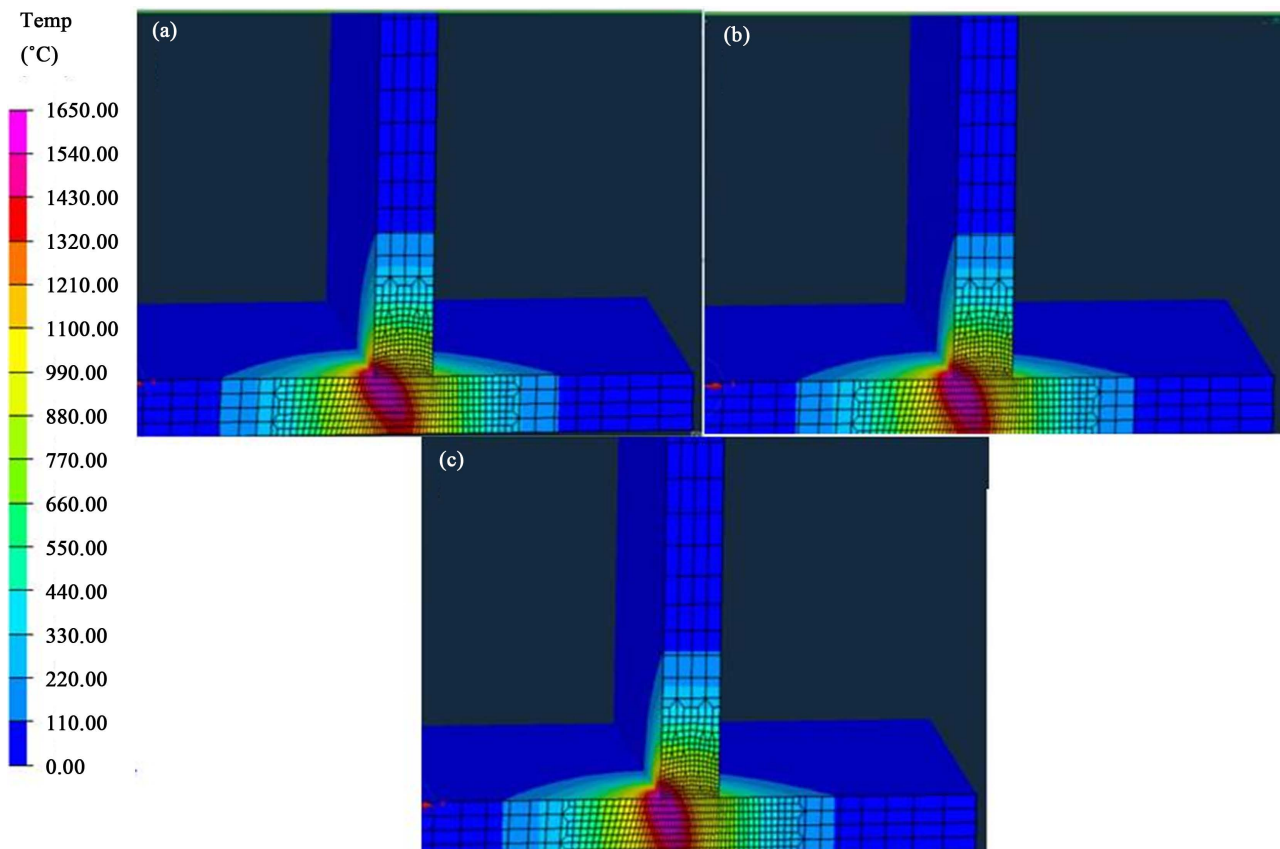


**Figure 3.** Variation in weld pool shape and angle, showing (a) the  $-8^\circ$  torch angle model; (b) the default model and (c) the  $+8^\circ$  torch angle model. (Images taken using Sysweld2014 computations and Visual Environment 9.5 post-processing software).

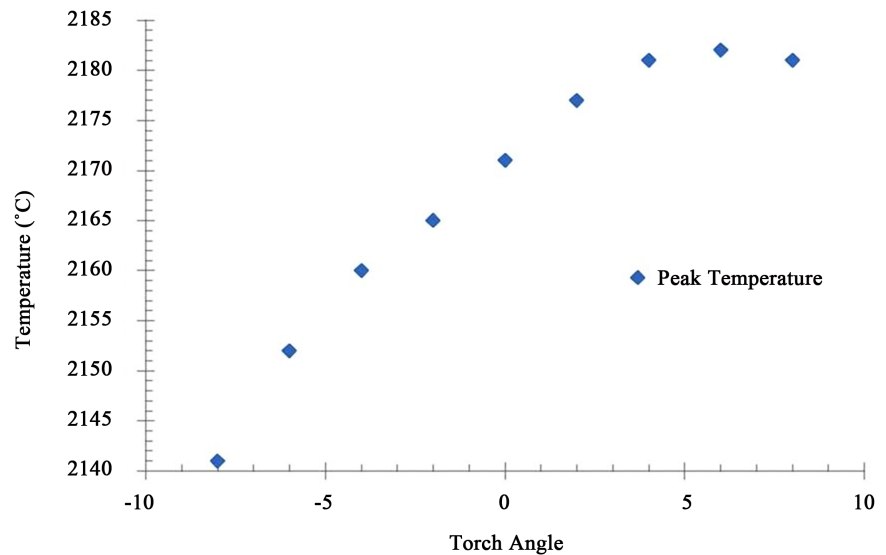


**Figure 4.** Graph displaying the sensitivity of predicted peak weld pool temperature to welding torch angle.

### 3.2. Distortion

Of greater interest is the mechanical response to the thermal loading. Recall that the models are all set-up identically, barring the torch angle, so all variations in mechanical response are solely due to this torch angle variation. Analysing the magnitude of distortion, clearly the overall distortion pattern remains similar across all models (see **Figure 5**). However the absolute value of peak distortion is greatest for a shallow angled torch, and reduces as the angles gets steeper.

Clearly, for the steeper torch angle, the depth of penetration in to the plate is slightly greater than that for a shallow angled torch. The maximum distortion predicted for the shallowest-angled weld along the edge of the horizontal plate is 0.456 mm, and this reduces to 0.432 mm for the steepest torch angle weld—see **Figure 6**. Whilst this is only a reduction in peak distortion of 0.024 mm, this does represent more than a 5% reduction overall, which may be significant given the precision/tolerance of welded components.

It is also significant to note the increasing distortion at the leading corner of the vertical plate in the T-joint arrangement considered here, as torch angle steepens. The distortion observed for the vertical plate was significant, with a 50% variation when comparing the shallowest and the steepest torch angle models—see **Figure 6**.

Hence, whilst globally maximum distortion is reducing with steeper torch angles, locally (at certain locations) the opposite trend is true. At this point on the vertical plate, a steeper torch angle with greater molten pool penetration is causing a larger distortion due to a larger volume of material below the intersection of the two plates undergoing thermal expansion as the weld torch moves along the path. Due to the process being autogenous, thus the lack of any reinforcing weld bead either side of the vertical plate will exacerbate the potential for the plate to deform and therefore tilt to one side or the other.

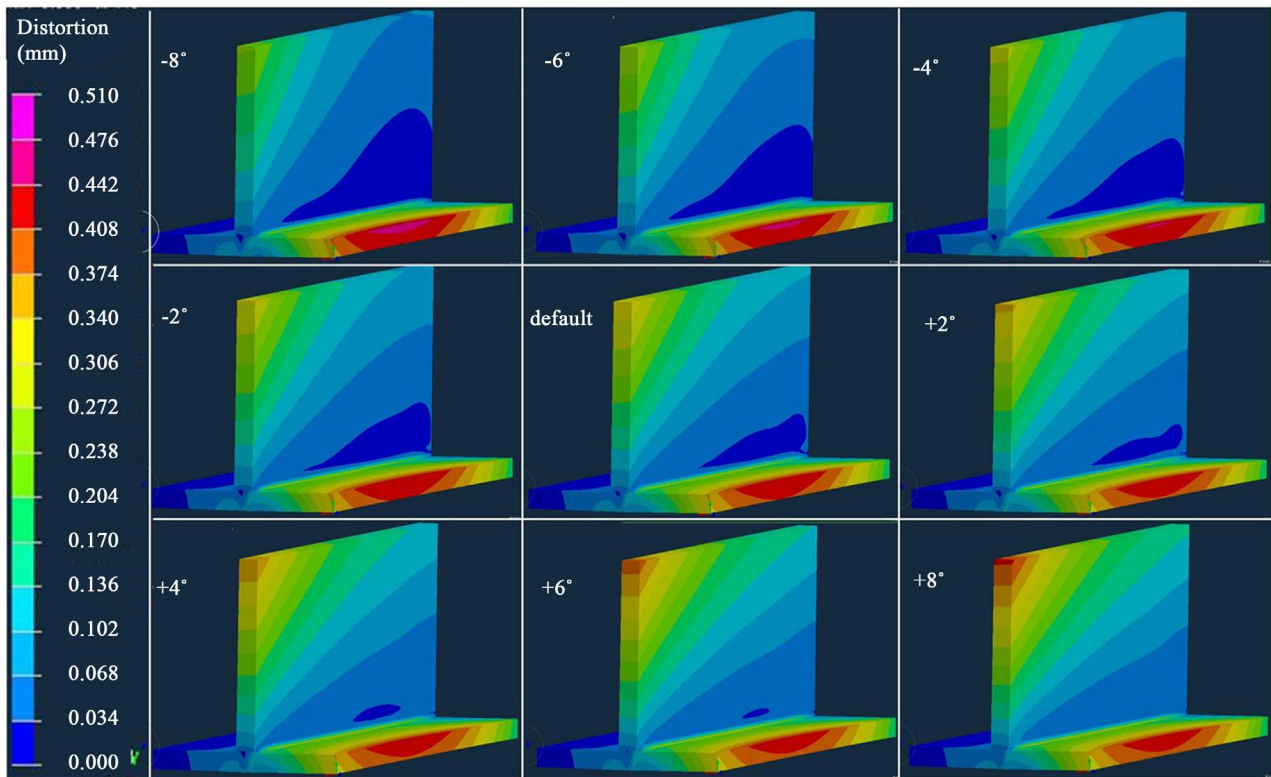


**Figure 5.** Total distortion fields as predicted by Sysweld for the 9 FE models varying the torch angle (images from Visual Environment 9.5 post-processing software).

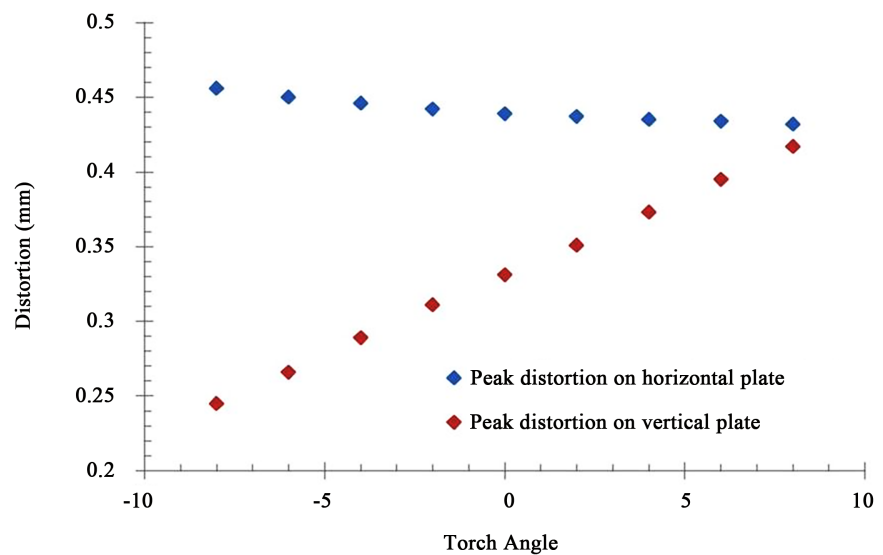


**Figure 6.** Graph illustrating the sensitivity of predicted peak distortions in both vertical and horizontal plates, to welding torch angle.

### 3.3. Residual Stress and Plastic Strain

Plastic strain distributions and Von Mises residual stress distributions have also been compared for the various nine parametric models. Given the relative similarity in results, only the images from the models representing a  $-8^\circ$  torch angle,

the default torch angle and the  $+8^\circ$  torch angle are displayed in **Figure 7**. Upon analysis, the predicted peak Von Mises residual stress displayed a clear trend for a reduction in Von Mises stress as the torch angle gets steeper—see **Figure 8**. However, this reduction is only of less than 1.5%, thus making the Von Mises residual stress very insensitive to variation in welding torch angle.

Whereas, the predicted peak plastic strain displays a clear trend of increasing as the welding torch angle becomes steeper—see **Figure 9**. The variation in plastic strain predicted by these models was of approximately 10%, suggesting that the plastic strain local to the weld line has some small sensitivity to torch angle, although certainly not the same level of sensitivity that the vertical plate distortion displayed.

**Table 3** summarises the overall impact of the  $\pm 8^\circ$  torch angle variation upon each of the considered outputs of temperature, distortions, Von Mises residual stress and plastic strain. As can be seen from the table, the overall sensitivities of the predicted outputs were all low, below approximately 10%, with the

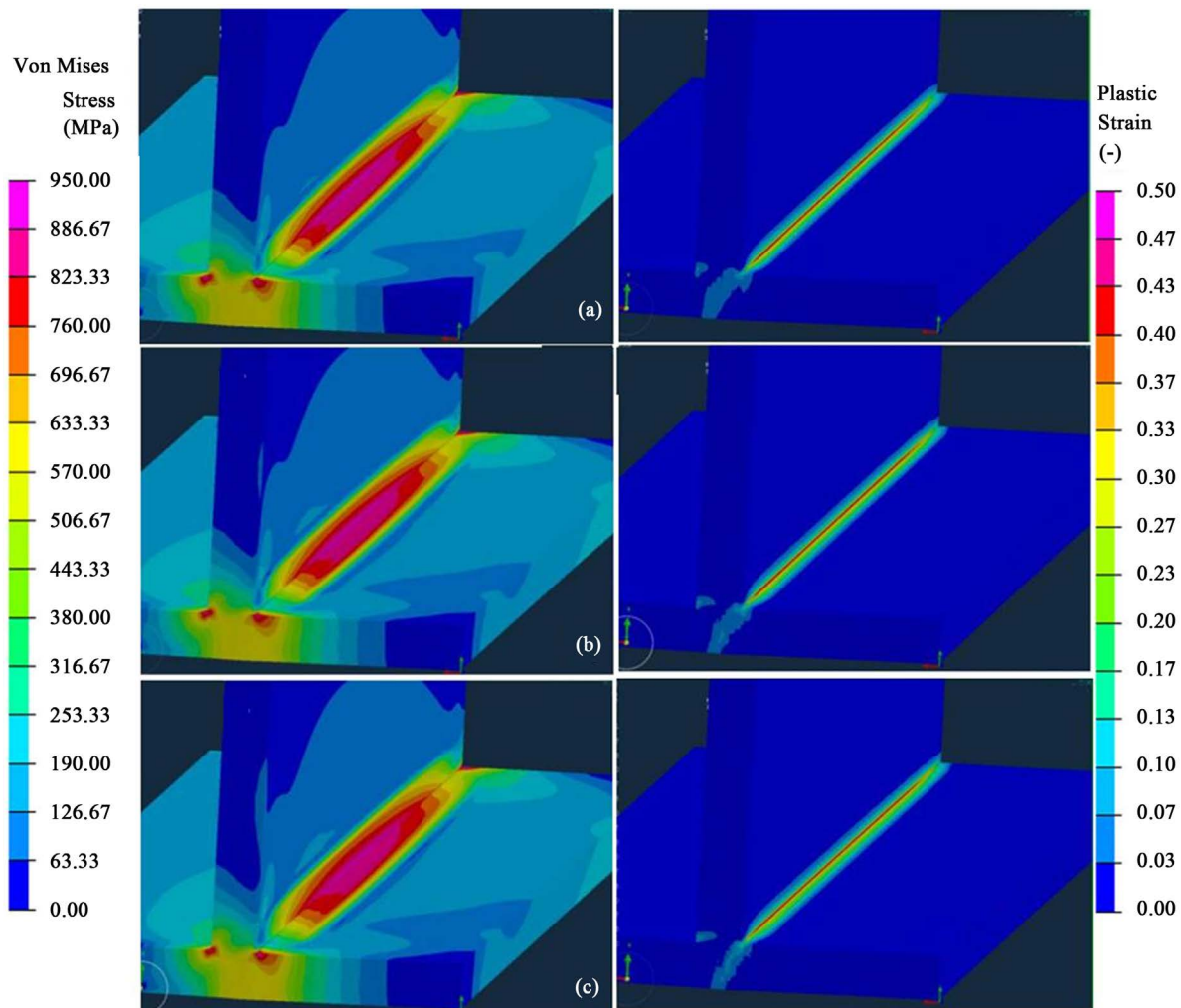


**Figure 7.** (left) Von Mises residual stress distribution, and (right) plastic strain distribution from the T-joint weld model with (a)  $-8^\circ$  torch angle; (b) default model; (c)  $+8^\circ$  torch angle (Images taken using Visual Environment 9.5 post-processing software).

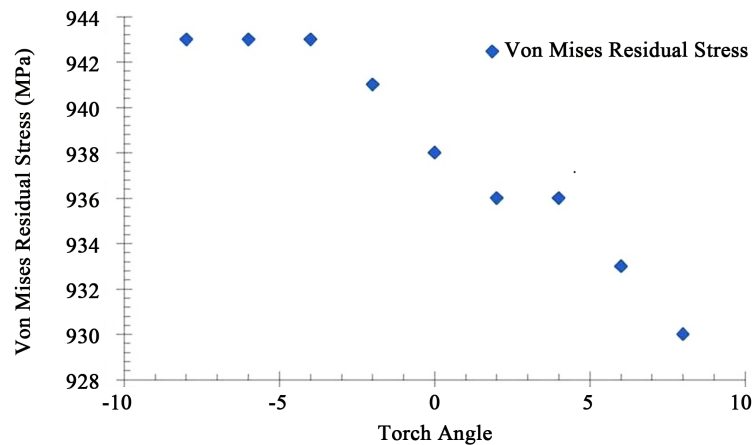


**Figure 8.** Graph illustrating sensitivity of predicted peak Von Mises residual stress to welding torch angle.

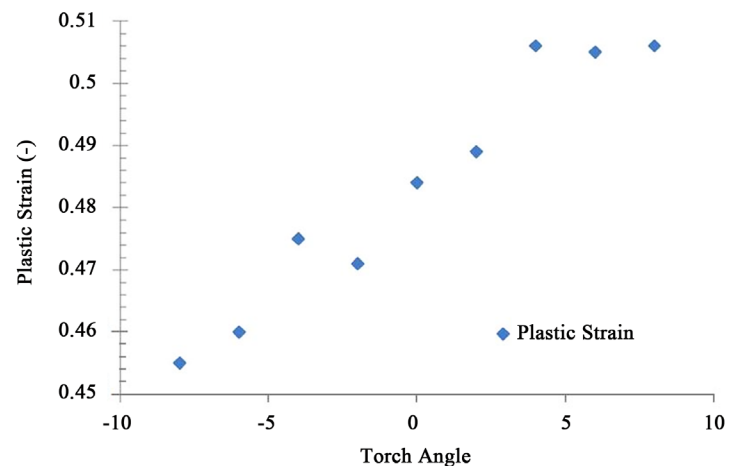


**Figure 9.** Graph illustrating sensitivity of predicted peak plastic strain to welding torch angle.

**Table 3.** Sensitivity of the considered outputs to torch angle.

FE output	Temperature	Horiz. plate distortion	Vertical plate distortion	Von Mises residual stress	Plastic strain
Max. Sensitivity	1.8%	5.5%	52.0%	1.4%	10.1%

exception of the distortions predicted on the vertical plate. Thus the modelling work suggests strongly that only the distortion for the vertical plate is sensitive to the torch angle inputted parameter.

#### 4. Conclusions

A parametric study of weakly coupled thermal and mechanical FE simulations of the TIG welding of a T-joint titanium alloy component have been calculated to study the effect of torch angle upon the welding outputs, where the only variable allowed between models was the torch angle. The following conclusions have been drawn:

- The change in temperature predicted by the parametric models is minimal, as expected. Variation in angle from  $-8^\circ$  to  $+8^\circ$  produces roughly 1.8% variation in peak temperature, which is expected to be purely a numerical effect caused by different integration points being heated.
- As the torch angle becomes steeper, the distortion observed on the horizontal plate reduces. A variation in torch angle from  $-8^\circ$  to  $+8^\circ$  produces a reduction in maximum predicted distortion of 5.5%.
- However, as torch angle becomes steeper, the distortion observed on the vertical plate increases dramatically, indicating a strong sensitivity. A variation in torch angle from  $-8^\circ$  to  $+8^\circ$  produces an increase in maximum predicted distortion of over 50%.
- The current modelling set-up sees the greatest distortion on the horizontal plate, for all models. However, for the steepest torch angle weld simulation, the absolute values of distortion for horizontal and vertical plate were close, and any greater variation in torch angle could see the location of the peak distortion move from one plate to another.
- Maximum plastic strain is predicted to be sensitive to welding torch angle, with a variation of approximately 10% in peak plastic strain for the torch angle variation in torch angle from  $-8^\circ$  to  $+8^\circ$  considered in this work.
- Von Mises residual stress is predicted to be highly insensitive to welding torch angle. Models show a variation of less than 1.5% in peak residual stress for the torch angle variation in torch angle from  $-8^\circ$  to  $+8^\circ$  considered in this work.

## Acknowledgements

This work was carried out as a part of the CASiM<sup>2</sup> collaborative project. The author thanks the funding body, ERDF, for financially supporting this project. Thanks are offered to ESI Group, distributors of the specialist welding FE code Sysweld2014, and its pre- and post-processor unit Visual Environment 9.5.

## References

- [1] Baghel, P.K. and Nagesh, D.S. (2017) Pulse TIG Welding: Process, Automation and Control. *Journal of Welding and Joining*, **35**, 43-48.
- [2] Henon, B.K. (2010) Automated Hot Wire TIG with Positioner for High Productivity Quality Welding. Focus on Nuclear Power Generation, February 2010.
- [3] Panchal, K. (2016) Experimental Investigation of TIG Welding on Stainless Steel and Mild Steel Plates. *Journal of Emerging Technologies and Innovative Research (JETIR)*, **3**, 25-32.
- [4] Lindgren, L.-E. (2006) Numerical Simulation of Welding. *Computer Methods in Applied Mechanics and Engineering*, **195**, 6710-6736.
- [5] Lundback, A. (2010) Finite Element Modelling and Simulation of Welding of Aerospace Components. Doctoral Licentiate Thesis, Lulea University of Technology, Sweden.
- [6] Villa, M. (2016) Metallurgical and Mechanical Modelling of Ti-6Al-4V for Welding

---

Applications. Ph.D. Thesis, University of Birmingham, UK.

- [7] Turner, R.P., Gebelin, J.-C., Ward, R.M., Huang, J. and Reed, R.C. (2012) Modelling of the Electron Beam Welding of a Titanium Aeroengine Compressor Disc. *Proceedings of the 9th International Trends in Welding Research Conference*, Chicago.
- [8] Stone, H.J., Roberts, S.M. and Reed, R.C. (2000) A Process Model for the Distortion Induced by the Electron Beam Welding of a Nickel-Based Superalloy. *Metallurgical and Materials Transactions A*, **31**, 2261-2273.
- [9] Ganjigatti, J.P., Pratihari, D.K. and RoyChoudhury, A. (2008) Modelling of the MIG Welding Process Using Statistical Approaches. *The International Journal of Advanced Manufacturing Technology*, **35**, 1166-1190.
- [10] Cho, D.-W. Cho, W.-I. and Na, S.-J. (2014) Modeling and Simulation of Arc: Laser and Hybrid Welding Process. *Journal of Manufacturing Processes*, **16**, 26-55.
- [11] Rosenthal, D. (1946) The Theory of Moving Sources of Heat and Its Application to Metal Treatments. *Transactions ASME*, **43**, 849-866.
- [12] Goldak, J., Chakravati, A. and Bibby, M. (1984) A New Finite Element Model for Welding Heat Sources. *Metallurgical Transactions B*, **15**, 299-305.  
<https://doi.org/10.1007/BF02667333>
- [13] ESI Group, 100-2 Avenue de Suffren, 75015 Paris, France.
- [14] Schmitz, G.J. (2012) Integrated Computational Materials Engineering: Concepts and Applications. Wiley & Sons, 179. <https://doi.org/10.1002/9783527646098>